EFFECTIVE VENTILATION

9th AIVC Conference, Gent, Belgium
12-15 September, 1988

Poster 7

# DEVELOPMENT OF AN EFFICIENT CONTROL ALGORITHM FOR A MULTIZONE CONSTANT CONCENTRATION TRACER GAS AIR INFILTRATION MEASUREMENT SYSTEM

R. COMPAGNON
A. KOHLER
C. ROECKER
C.-A. ROULET

Laboratoire d'Energie Solaire et de Physique du Bâtiment
LESO-PB
Ecole Polytechnique Fédérale de Lausanne
CH - 1015 Lausanne
SWITZERLAND

## ABSTRACT

A constant concentration tracer gas (CCTG) measuring system needs a control algorithm to calculate, at each sampling time, the required tracer gas injection rate to keep the gas concentration at a target level. A new control algorithm is presented here in full details. Practical considerations concerning modifications to take into account the physical limitations of the CCTG system and the computing of the optimal control parameters are also presented.


## 1. INTRODUCTION

The constant concentration tracer gas technique (CCTG) is now commonly used for air flow measurement within buildings. This technique requires a control algorithm to keep the gas concentration at a target level by computing the necessary amount of tracer gas to inject. In an inhabited multizone building, the control algorithm has to respond quickly to large variations of interzonal airflows and/or outside air infiltration.

Few authors[1,2,3] have described in detail the implemented algorithm of their CCTG systems. As far as we know, they all use common control methods such as P, PI or PID.

We present a different control algorithm, used on our CESAR* system[4,8]. In order to improve this control method, we developed a computer program simulating a room with variable air change rate which takes the real characteristics of the CCTG system into account. This program allowed us to test some modifications of the theoretical control algorithm and to estimate its optimal parameters.

* CESAR : Compact Equipment for Survey of Air Renewal.

## 2. THEORETICAL APPROACH

### 2.1 Single zone model

In a first step, we consider a single zone. The equation governing the tracer gas concentration into the zone is :

$$V\frac{dC}{dt} = -FC + S \qquad (1)$$

where V : effective volume of the zone [$m^3$]

C : tracer gas concentration [-]

F : air flow leaving the zone [$\frac{m^3}{s}$]

S : tracer gas injection into the room [$\frac{m^3}{s}$]

This equation assumes that the outside tracer gas concentration is negligible and that the air has a constant density. A perfect mixing of the tracer gas within the zone is also assumed. Even if these assumptions are not always true in real conditions, this model is sufficiently good for control purposes.

Since the CCTG system analyses the concentrations in the zone by sampling at discrete time, the differential equation (1) should be integrated over one sampling time $T_s$ to give a difference equation :

$$C_{k+1} = a_k C_k + b_k U_k \qquad (2)$$

where : $C_{k+1}, C_k$ : tracer gas concentration at time $(k+1)\,T_s$ and $kT_s$ respectively [-]

$U_k = \frac{S_k}{V}$ : injection rate $[\frac{1}{s}]$

$$a_k = \exp\left(-\frac{F_k}{V} \cdot T_s\right) \quad [-] \qquad (3)$$

$$b_k = V\left(\frac{1 - a_k}{F_k}\right) \text{ if } F_k > 0,\ b_k = T_s \text{ if } F_k = 0 \quad [s] \qquad (4)$$

$T_s$ : sampling time [s]

$k$ : sample number [-]

The air flow $F_k$ and the injection rate $S_k$ are assumed to be constant over the integrating time interval $(k\,T_s; (k+1)\,T_s)$.

## 2.2 Control algorithm

The function of the control algorithm is to compute the necessary injection rate $U_k$ to maintain the concentration at a target level denoted $W_k$ (for complete generality the target level may also change during time : therefore it is also denoted by the sample number k). The injection rate is computed using the expression :

$$U_k = -K_s C_k + K_R X_{Rk} + K_w W_k \quad [s^{-1}] \qquad (5)$$

with $K_s, K_R, K_w$ : parameters of the control algorithm $[s^{-1}]$

$X_{Rk}$ : an integrating term defined by the difference equation :

$$X_{Rk+1} = X_{Rk} + W_k - C_k \quad [-] \qquad (6)$$

This expression is derived by minimizing the quadratic form :

$$J = \sum_{k=0}^{\infty} [(W_k - C_k)\, Q_e\, (W_k - C_k) + X_{Rk}\, Q_R\, X_{Rk} + U_k\, R\, U_k] \qquad (7)$$

where $Q_e$, $Q_R$ and R are weighting factors (see [5] for full details).

Different methods are available for the determination of the parameters $K_s$ $K_R$ and $K_w$. We choose a method which consists of imposing the poles of the system[5]. This method is far more practical to use for two reasons :

- It is not necessary to make an arbitrarily choice of the weighting factors for the quadratic form

- The computing of $K_s$, $K_R$ and $K_w$ is easier and doesn't require complex computer code as the other methods.

In fact the two poles of the system depend only on the parameters $K_s$ and $K_R$. The value of the third parameter $K_w$ doesn't have any influence on the pole location but may be used to compensate the effect of one pole.

The relations between the poles and the parameters are :

First case : Real poles $Z_1$ and $Z_2$ ($Z_1$, is the compensated pole)

$$K_s = \frac{- Z_1 - Z_2 + a_k + 1}{b_k} \qquad [\frac{1}{s}] \tag{8}$$

$$K_R = \frac{(1 - Z_1)(1 - Z_2)}{b_k} \qquad [\frac{1}{s}] \tag{9}$$

$$K_w = \frac{K_R}{1 - Z_1} \qquad [\frac{1}{s}] \tag{10}$$

Second case : Two complex conjugate poles $Z_{1,2} = \mathrm{Re}(Z) \pm i \, \mathrm{Im}(Z)$
(the real part of the pole is compensated)

$$K_s = \frac{(- 2 \,\mathrm{Re}(Z) + a_k + 1)}{b_k} \qquad [\frac{1}{s}] \tag{11}$$

$$K_R = \frac{((\mathrm{Re}(Z) - 1)^2 + \mathrm{Im}^2(Z))}{b_k} \qquad [\frac{1}{s}] \tag{12}$$

$$K_w = \frac{K_R}{1 - \mathrm{Re}(Z)} \qquad [\frac{1}{s}] \tag{13}$$

where $a_k$ and $b_k$ are defined by (3) and (4).

Through $a_k$ and $b_k$ the parameters are functions of the sampling time $T_s$ and of the air change rate $\frac{F_k}{V}$. There is apparently a problem here as the control algorithm requires parameters which depend on the varying air change rates not known before measurement ! In fact the control algorithm needs only an estimation of the air change rate and the parameters are calculated once for the entire measurement procedure. This point and the optimal location of the poles will be discussed further in chapter 3.

At the beginning of the measurement procedure, the integrating term $X_{Rk}$ has to be initialized to a certain value. Under the assumption that the initial concentration Co was kept constant in the past, the initial value $X_{Ro}$ is defined by :

First case : Real poles $Z_1$ and $Z_2$ ($Z_1$ is the compensated pole)

$$X_{Ro} = \frac{1}{1 - Z_2} \cdot C_o \tag{14}$$

Second case : Two complex conjugate poles (the real part of the poles is compensated)

$$X_{Ro} = \frac{1}{1 - \text{Re}\,(Z)} \cdot C_o \tag{15}$$

## 2.3 Advantages of the algorithm

The proposed control algorithm defined by equation (5) looks like a special case of a traditional PI control algorithm. In fact our algorithm present some advantages over the usual PI control method.

First, a faster response to a step change in the target concentration $W_k$ is obtained by the pole compensation (Fig. 1). This property is very useful for measurement procedures using variable target concentrations in multizone buildings.

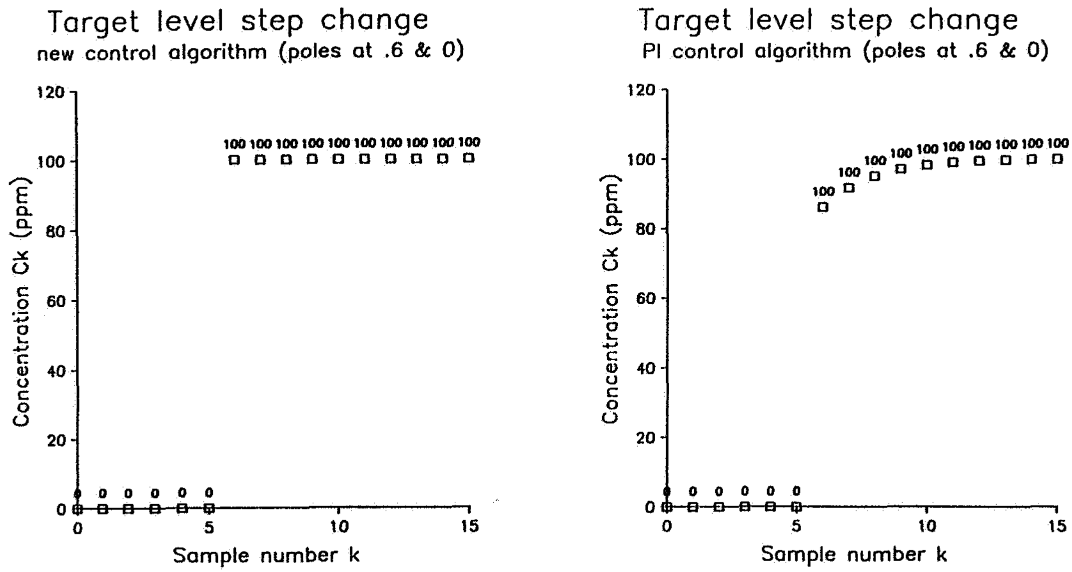


Figure 1 : Response of the control algorithm for a target level step change : the new control algorithm has a faster response than the PI control method. Points are labelled by the actual target level $W_k$ (ppm). (values computed with 1 air change/hour and $T_s = 540$ [s]).

Secondly, the minimization of a quadratic form is well suited to generalize into a multivariable control algorithm. Thus an extension of our algorithm to the case of a multizone measurement system is not difficult. This extension is summarized as follows : equation (1) is rewritten[6] using matrix notation :

$$\mathbf{V} \frac{d}{dt} \mathbf{C} = \mathbf{F}\ \mathbf{C} + \mathbf{S} \tag{16}$$

where

| | | | |
|---|---|---|---|
| where | $\mathbf{V}$ : | volumes diagonal matrix | $[m^3]$ |
| | $\mathbf{C}$ : | concentrations vector | [-] |
| | $\mathbf{F}$ : | air flows matrix | $[\frac{m^3}{s}]$ |
| | $\mathbf{S}$ : | tracer gas injections vector | $[\frac{m^3}{s}]$ |

The difference equation (2) becomes :

$$\mathbf{C}_{k+1} = \mathbf{A}\ \mathbf{C}_k + \mathbf{B}\ \mathbf{U}_K \qquad (17)$$

where **A** and **B** are matrixes derived from the air flows matrix **F** and the volumes matrix **V**

and $$\mathbf{U}_k = \mathbf{V}^{-1}\ \mathbf{S}_k \qquad (18)$$

From equation (17), various methods are available[5] to compute the parameters matrixes $\mathbf{K}_s$,$\mathbf{K}_R$ and $\mathbf{K}_w$ necessary for the control algorithm defined (similar to equation (5) by :

$$\mathbf{U}_k = -\ \mathbf{K}_s\ \mathbf{C}_k + \mathbf{K}_R\ \mathbf{X}_{Rk} + \mathbf{K}_w\ \mathbf{W}_k \qquad (19)$$

where $\mathbf{W}_k$ is the target concentrations vector and $\mathbf{X}_{Rk}$ the integrating vector defined by the difference equation :

$$\mathbf{X}_{Rk+1} = \mathbf{X}_{Rk} + \mathbf{W}_k - \mathbf{C}_k \qquad (20)$$

## 2.4 Modifications of the algorithm

The tracer gas injection rate the CCTG is able to supply is limited to a certain range : no tracer gas can be removed from the zone and, a maximum injection rate can not be exceeded. Figures 2 and 3 show two cases where these limitations lead to large over- or under-shoots of concentration.

These problems are caused by inappropriate values of the integrating term $X_{Rk}$. Although the CCTG system cannot supply the necessary injection rate or remove gas to readjust the concentration to target level, the value of $X_{Rk}$ is still incremented as if the system had no limitations. This results in too high or too low values of $X_{Rk}$, and it takes several steps with over or under concentration to correct the value of this term.

To avoid these problems, it is necessary to correct the value of $X_{Rk}$ when the system is unable to supply the injection rate the control algorithm has asked for. Among the many possibilities to adjust these values, we present here two procedures we have chosen :

First case : $U_k < 0$

Negative values typically occur after a concentration overshoot due to an abrupt decrease of the air infiltration rate into the zone (Fig. 2). As seen above (equation 5), the injection rate is proportional to $W_k$, - $C_k$ and $X_{Rk}$. During the whole overshoot while $C_k > W_k$, the integrating term decreases. Then, when the concentration goes below the target level, because of the low value of $X_{Rk}$, the injection rate remains negative and it takes several steps with $C_k < W_k$ to raise the value of $X_{Rk}$ to its new stationary value allowing positive injection rate to be computed.

To avoid this undershooting, the integrating term could be adjusted just before the decreasing concentration crosses the target level. Thus, our procedure works as follows :

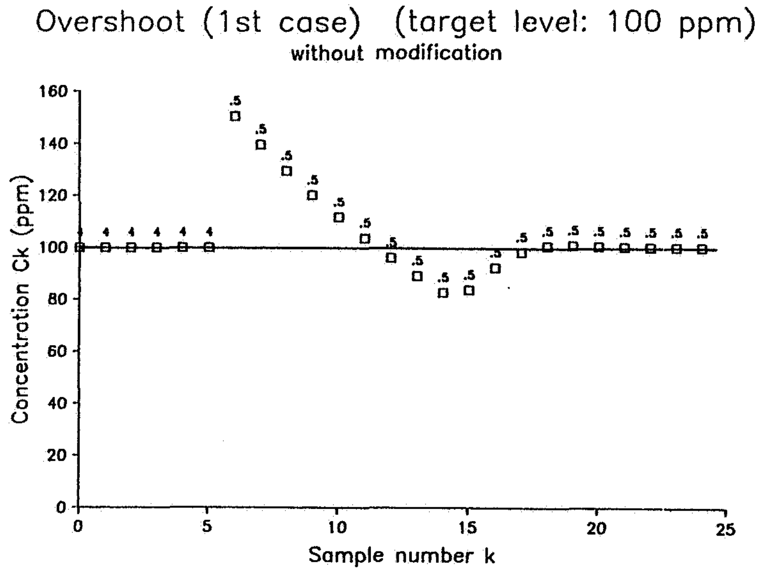


**Figure 2 :** Concentration overshoot due to an abrupt decrease of the air change rate. Points are labelled by the actual air change rate [$h^{-1}$] (values computed with $V = 80$ [$m^3$] and $T_s = 540$ [s]).

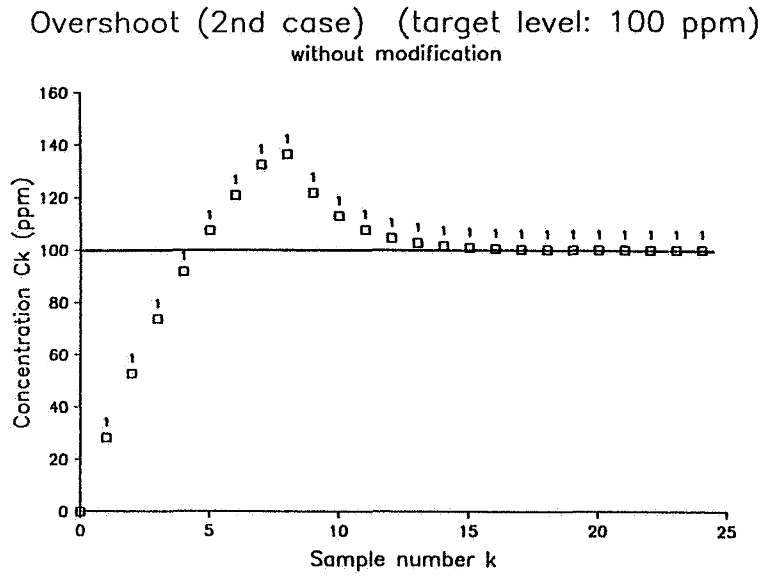


**Figure 3 :** Concentration overshoot due to the limiting effect of the maximum injection rate $U_{max}$ the CCTG system is able to supply. All points are labelled by the actual air change rate [$h^{-1}$] (values computed with $V = 200$ [$m^3$], $T_s = 540$ [s] and $U_{max} = 5.67 \cdot 10^{-8}$ [$s^{-1}$]). These values lead to the maximum concentration increase at the first step : $C_1 = b \cdot U_{max} = 28{,}4$ (ppm)).

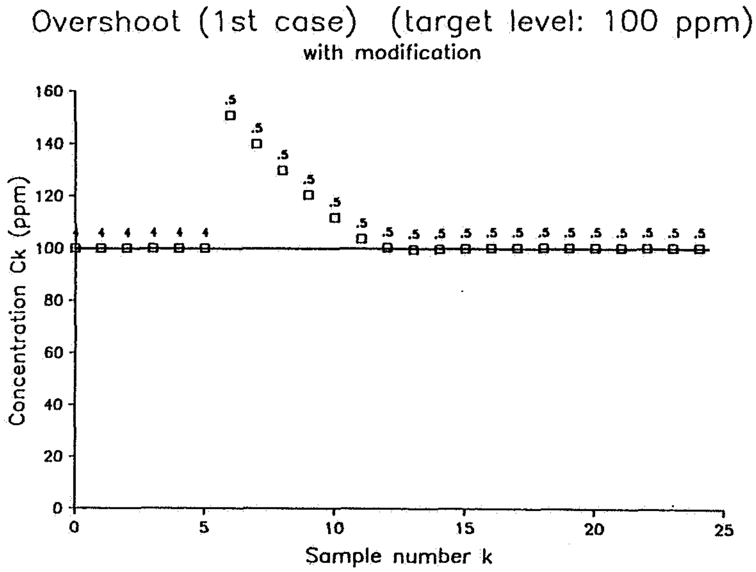


**Figure 4 :** Effect of the first modification of the control algorithm (compare with fig. 2). All points are labelled by the actual air change rate [$h^{-1}$]. (values computed with $V = 80$ [$m^3$] and $T_S = 540$ [s]).

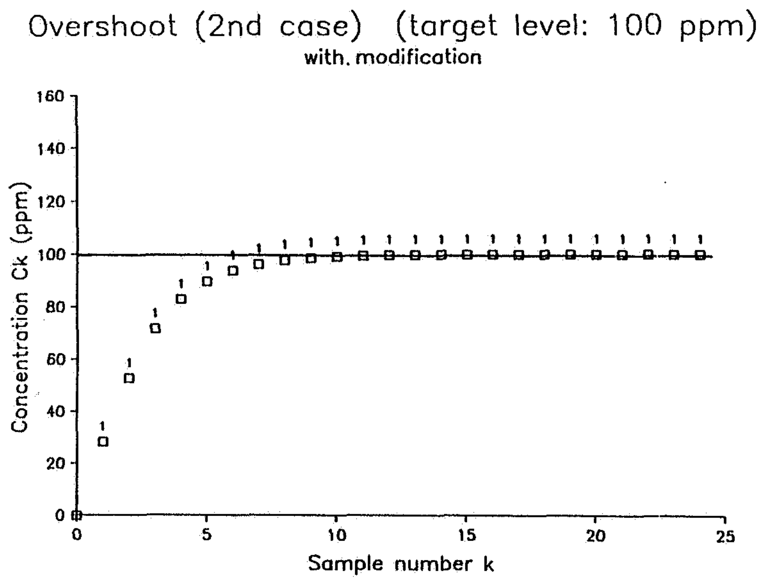


**Figure 5 :** Effect of the second modification of the control algorithm (compare with fig. 3). All points are labelled by the actual air change rate [$h^{-1}$] (values computed with $V = 200$ [$m^3$], $T_S = 540$ [s] and $U_{max} = 5.67 \cdot 10^{-8}$ [$s^{-1}$]).

Whenever the control algorithm computes a negative injection rate, the actual infiltration rate is estimated and the concentration for the next step can be extrapolated. If, without any gas injection, the extrapolated concentration is still above target level, nothing is done. But in the other cases, the integrating term is forced to a value leading, through the use of control equation (5), to the necessary injection rate to reach the target level. The following relations are used for this procedure :

(assuming $U_k < 0$)

estimated actual air change rate :

$$n_{est} = \frac{1}{T_s} \cdot Ln\left(\frac{C_{k-1} + T_s \cdot \max\ (0;\ U_{k-1})}{C_k}\right) \quad [\frac{1}{s}] \qquad (21)$$

(if $U_{k-1} > 0$ $\quad n_{est}$ underestimates the true air change rate)

predicted concentration :

$$C_{p\ k+1} = C_k \exp\ (-n_{est} \cdot T_s) \quad [-] \qquad (22)$$

necessary injection rate (if $C_{p\ k+1} < W_{k+1}$) :

$$U_k^* = \frac{1}{T_s} C_k \left(\frac{W_{k+1}}{C_{p\ k+1}} - 1\right) \quad [\frac{1}{s}] \qquad (23)$$

new value for the integrating term :

$$X_{Rk}^* = \frac{U_k^* + K_s\ C_k - K_w\ W_k}{K_R} \quad [-] \qquad (24)$$

Since the actual air change rate is computed over one sampling time only, its value is sensitive to any measurement error. Therefore equation (23) gives in fact an underestimate of the necessary injection rate to avoid large effects from small measurement errors (it is always easier to add some gas at the next step than to remove some !).

A comparison between fig. 2 and fig. 4 shows the effect of this procedure.

Second case $U_k > U_{max}$

This case may occur at the beginning of a measurement on a large zone or when the air infiltration rate is very high. For extreme cases, the target concentration will never be reached.

Figure 3 illustrates the problem : the increase of the concentration is limited by $U_{max}$ while the integrating term increases. When the concentration reaches the target level, the high integrating term value forces the control algorithm to inject too much gas. This leads to a concentration overshoot until the integrating term finds its stationary value again.

To avoid this phenomenon, each time the control algorithm asks for an injection rate higher than $U_{max}$, the integrating term is forced to a proper value. This value is calculated so that, when used in the control equation (5), the maximum possible injection rate $U_{max}$ results.

The new value of the integrating term is then :

(assuming $U_k > U_{max}$)

$$X_{Rk}^{*} = \frac{U_{max} + K_s C_k - K_w W_k}{K_R} \quad [-] \qquad (25)$$

As shown in figure 5, this procedure gives good results.

## 3. ALGORITHM TESTING

### 3.1 Simulation program

In order to test the algorithm, a simulation program was developed[7]. The program simulates a zone with variable air change rate and takes into account the real characteristics of the CCTG system (e.g. time delays due to the pipes, gaz analyzer response time, random errors on the measured concentration, and maximum injection rate $U_{max}$).

The tracer gas mixing process within the zone is also simulated using a simple model : The tracer gas is injected in a small fictious volume which is connected to the zone by a constant air flow rate. The small fictious volume and the zone volume are both assumed perfectly mixed. A good mixing into the zone is achieved when the concentration within the fictious volume is close enough to the concentration within the zone. The mixing time constant is defined by :

$$\tau_{mx} = \frac{v}{f} \; [s] \qquad (26)$$

| | | | |
|---|---|---|---|
| where | v : | fictious volume | $[m^3]$ |
| | f : | constant air flow between the fictious volume and the zone | $[\frac{m^3}{s}]$ |

According to Sandberg and Blomqvist[3], this time constant typically lies between 30 [s] and 180 [s]. It can be adjusted by giving proper values to v and f. By assuming f equal to the flow rate produced by the small mixing fan used in the zone ($f \cong 0{,}015 \; [\frac{m^3}{s}]$ for the fans we use) the fictious volume lies in the interval between 0,45 and 2,7 $[m^3]$.

## 3.2 Results

Chapter 2 describes the control algorithm but gives no information on the location of the poles and the estimated air change rate. They are both required to compute the three parameters $K_s$ $K_R$ and $K_w$. To investigate these topics, we used our program to systematically try all the possible poles locations for different estimated air change rates. All simulations were performed under the operating conditions listed in table 1.

| | | | | |
|---|---|---|---|---|
| Sampling time | $T_s$ | $= 540$ | [s] | |
| Volume of the zone | V | $= 80$ | [$m^3$] | |
| Initial concentration | $C_o$ | $= 0$ | (ppm) | |
| Target concentration | W | $= 100$ | (ppm) | |
| Fictious volume | v | $= 0.9$ | [$m^3$] | $\}$ $\tau_{mx} = 60$ [s] |
| Air flow induced by the fan | f | $= 0.015$ | $[\frac{m^3}{s}]$ | |
| Measurement random error | gaussian noise | | $\mu = 0$ (ppm) | |
| | | | $\sigma = 1$ (ppm) | |
| Time delays due to the pipes | 5.2 [s] | | | |
| Analyzer response time | 8 [s] | | | |
| Maximum injection rate | $U_{max} = 1.42 \cdot 10^{-7}$ $[\frac{1}{s}]$ | | | |

Table 1 : Operating conditions used for our simulations.

To remain close to the conditions observed in inhabited buildings, the simulations were performed over 320 samples ($320 \cdot 540$ [s] = 48 hours) with variable air change rates as shown in fig. 6.

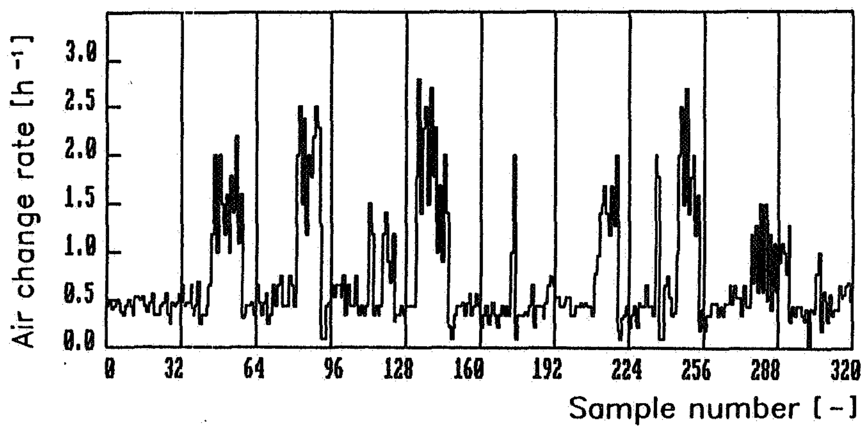


Figure 6 : Variable air change rate used for our simulations.

The simulations results were characterized by three numbers :

a) the difference between the mean measured concentration and the target level :

$$d = \langle C \rangle - W \qquad [-] \qquad (27)$$

b) the concentration standard deviation from the target level :

$$s = \sqrt{\langle (C - W)^2 \rangle} \qquad [-] \qquad (28)$$

c) the total negative tracer gas volume the control algorithm wanted to remove from the zone :

$$v_{neg} = V \cdot T_s \cdot \sum_{k=1}^{320} \min(0; U_k) \qquad [m^3] \qquad (29)$$

($\langle\,\rangle$ denotes the "mean" operator $= \frac{1}{N} \sum_{k=1}^{N}$ with N the number of samples)

It is clear that the optimal control algorithm would lead to ($d = 0$, $S = 0$, $v_{neg} = 0$) ! The set of simulations can then be investigated to find out the poles location leading to the smallest vector ($d$, $s$, $v_{neg}$). Figures 7 to 12 present different maps showing the values $d$, $s$ and $v_{neg}$ for all locations of the poles in real and complex planes.

By studying the maps, in the complex plane (fig. 7 to 9) no complete overlapping appears for the best regions for $d$, $s$ and $v_{neg}$. Therefore it is not advisable to locate the poles somewhere in the complex plane.

In the real plane (fig. 10 to 12), the three best regions lie closer to each other. We choose the poles location $Z_1 = 0{,}6$ (compensated pole) and $Z_2 = 0$ as the "best" values to compute the parameters of our algorithm.

It also appeared that the estimated air change rate required to compute the parameters has only a small influence on the simulation results. It is possible to understand this by looking at figure 13 which shows the dependance of the parameters from the estimated air change rate.

Parameter $K_w$ is the most sensitive parameter but it does not have a strong influence because the dynamic properties of the control algorithm are essentially determined by $K_s$ and $K_R$ which are much less sensitive to the estimated air change rate. It is anyhow important to keep in mind that $K_w$ has a strong influence when a target level step change occurs (e.g. at the beginning of the measurement procedure). It is therefore advisable to choose the minimum expected air change rate for the considered zone.

These conclusions still apply in case of bad mixing ($\tau_{mx} = 180$ [s]) and for other sets of air change rates if their values lie between 0 and 4 [$h^{-1}$]. For larger variations of air change rates, a recalculation of the control parameters should sometimes be undertaken during the measurement. This procedure and the criteria to apply it, will be investigated during the continuation of this work.

Figure 14 shows the concentrations during 12 hours of a real CCTG measurement using our algorithm with poles located at $Z_1 = 0{,}6$ $Z_2 = 0$, with an estimated air change rate of 0.1 [$h^{-1}$]. A fast response to changes in air flow rates can be observed.

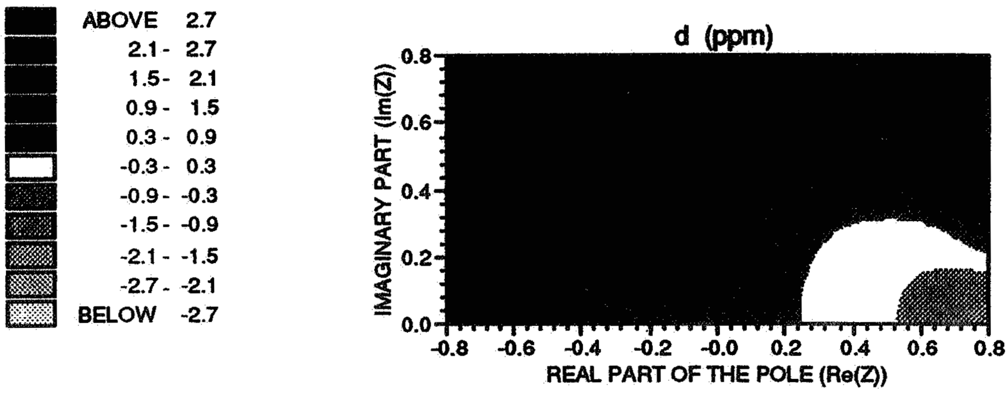


Figure 7 : Difference between the mean measured concentration and the target level in (ppm) for poles located in the complex plane. (Estimated air change rate used for the calculation of the control parameters : 0.5 [$h^{-1}$]).

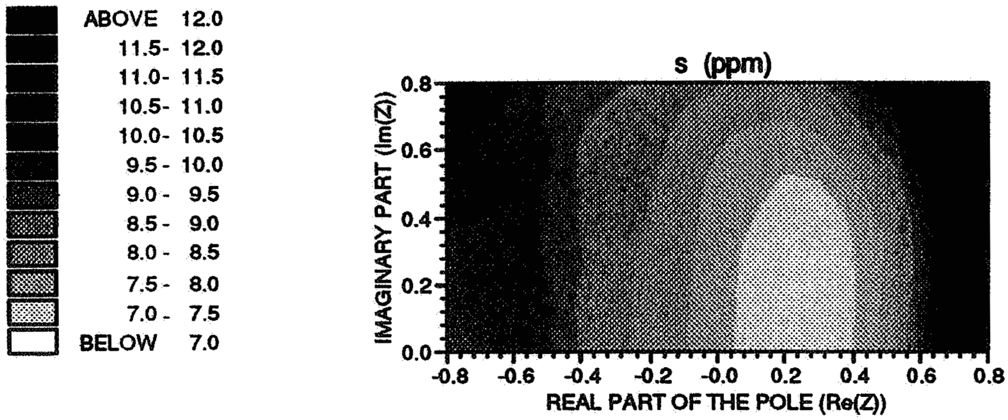


Figure 8 : Concentration standard deviation from the target level in (ppm) for poles located in the complex plane. (Estimated air change rate used for the calculation of the control parameters : 0.5 [$h^{-1}$]).

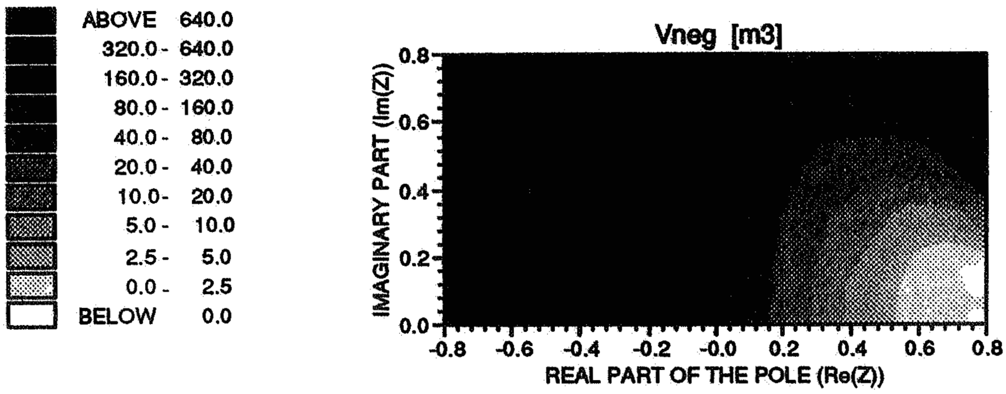


Figure 9 : Total negative tracer gas volume the control algorithm wanted to remove from the zone for poles located in the complex plane. (Estimated air change rate used for the calculation of the control parameters : 0.5 [$h^{-1}$]).

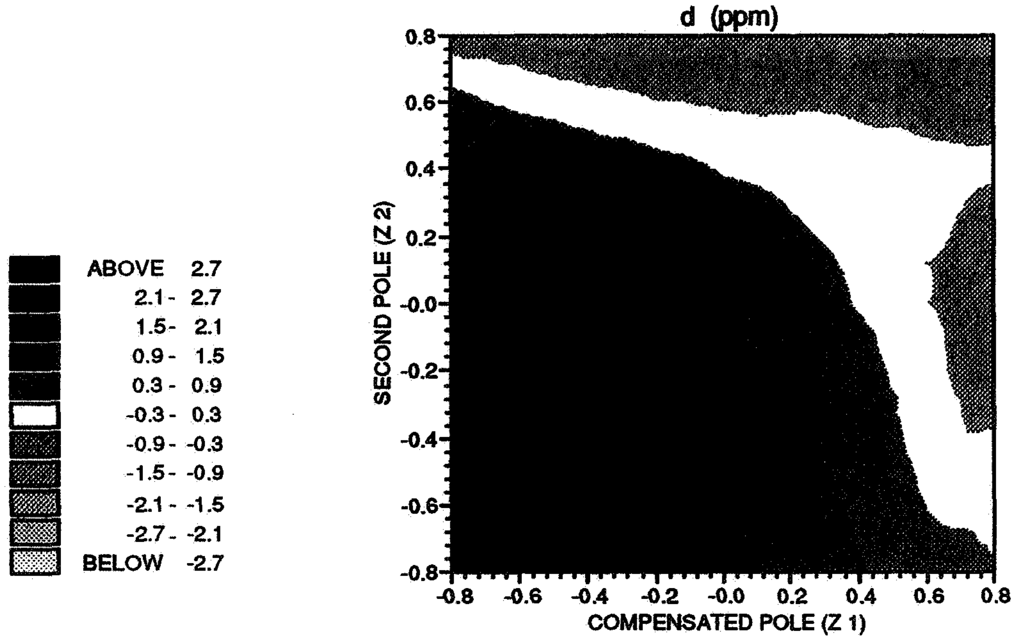


Figure 10 : Difference between the mean measured concentration and the target level in (ppm) for poles located in the real plane. (Estimated air change rate used for the calculation of the control parameters : 0.5 [$h^{-1}$]).

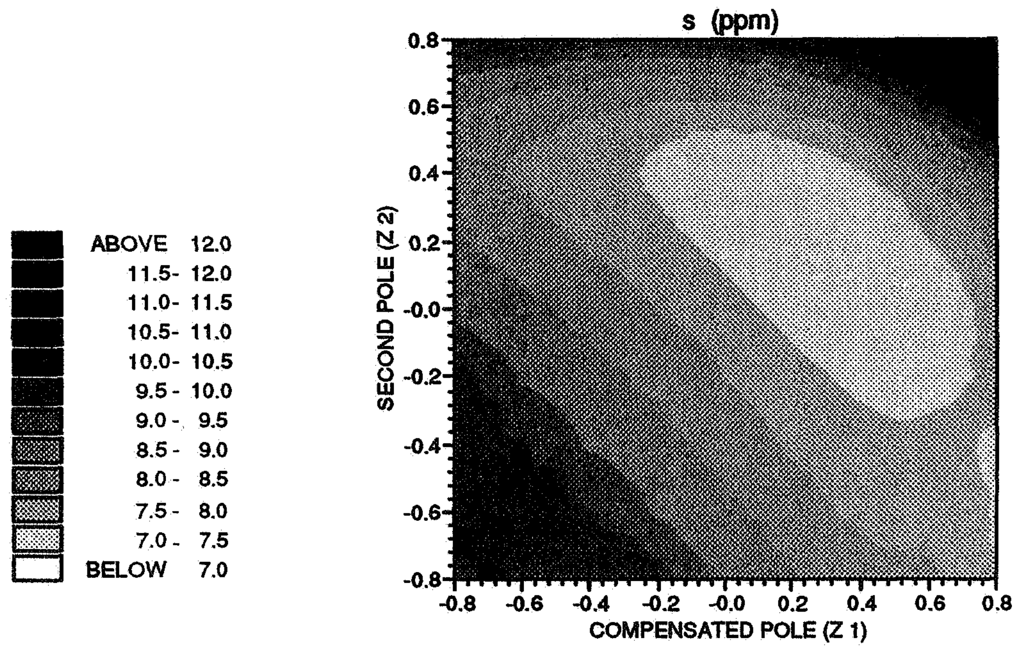


Figure 11 : Concentration standard deviation from the target level in (ppm) for poles located in the real plane. (Estimated air change rate used for the calculation of the control parameters : 0.5 [$h^{-1}$]).

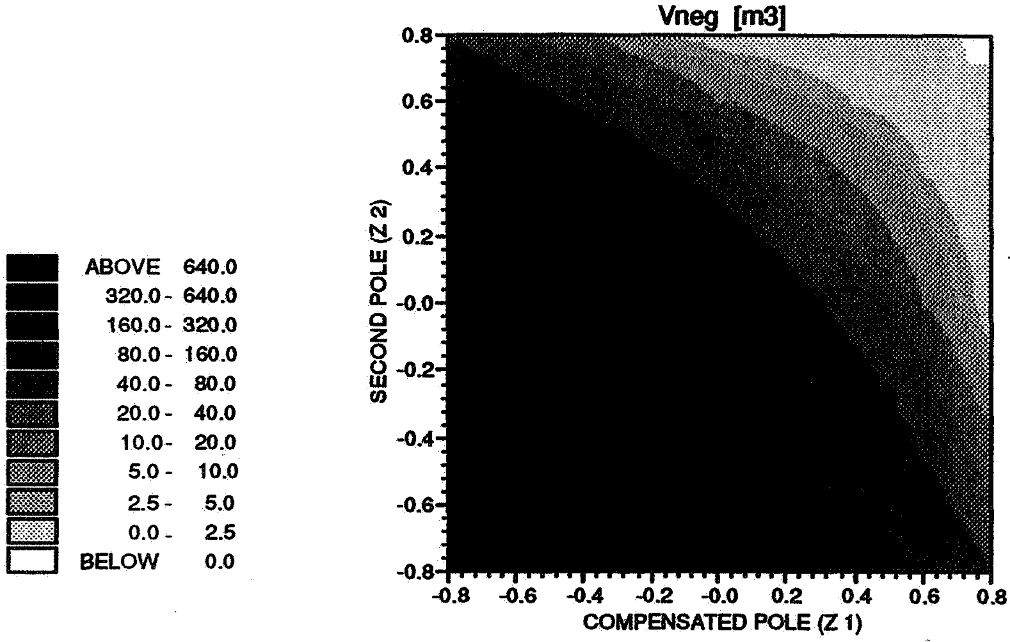


Figure 12 : Total negative tracer gas volume the control algorithm wanted to remove from the zone for poles located in the real plane. (Estimated air change rate used for the calculation of the control parameters : 0.5 [$h^{-1}$]).

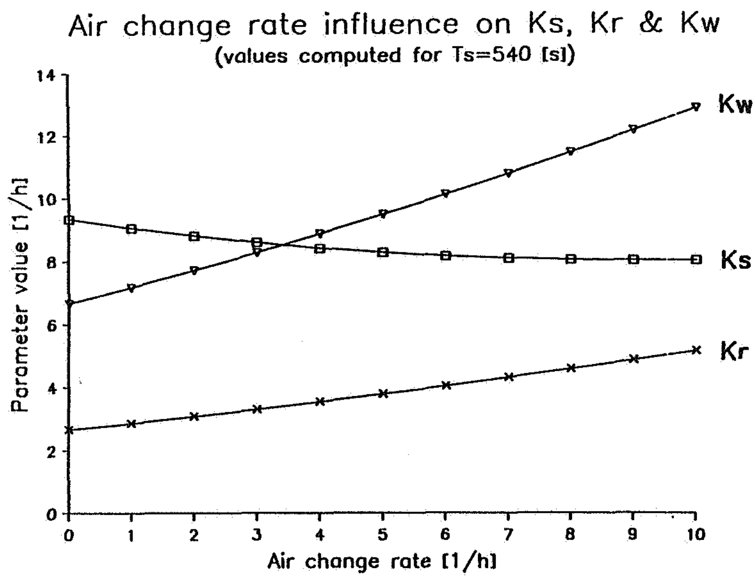


Figure 13 : Values (expressed in [$h^{-1}$]) of the control parameters for various estimated air change rates (poles located at $Z_1 = 0.6$ and $Z_2 = 0$).

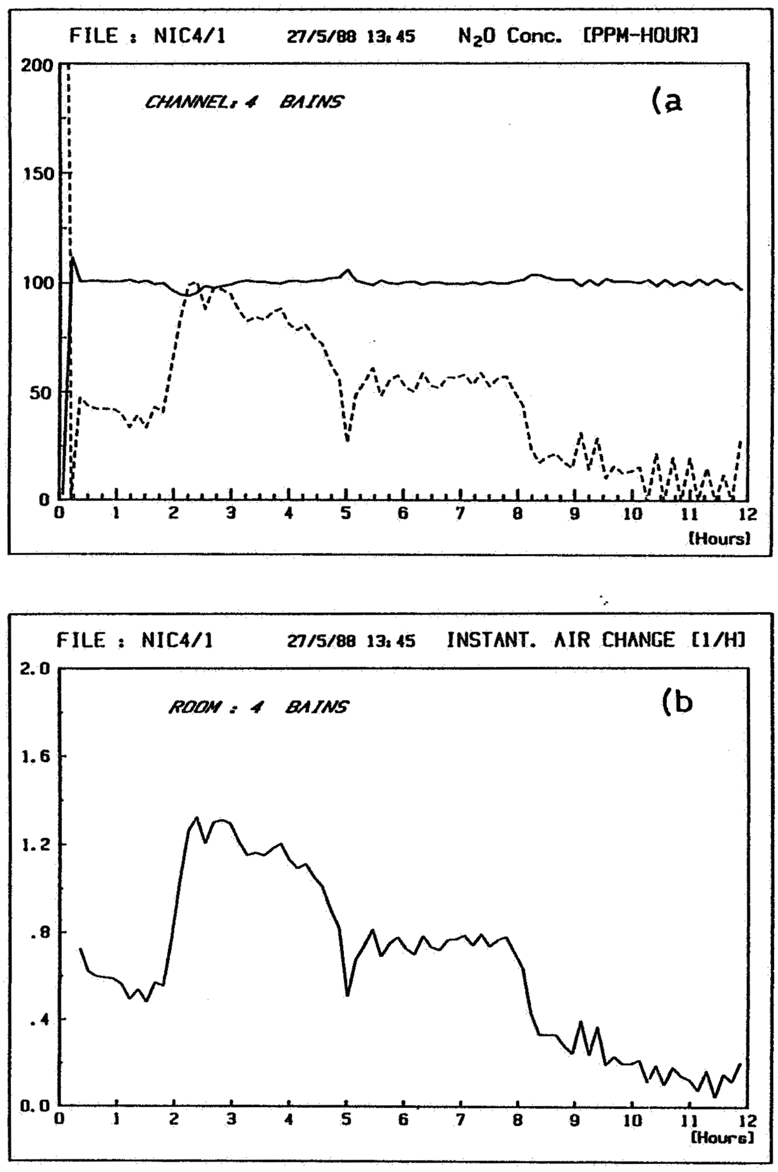


Figure 14 :

a) Concentrations measured during 12 hours within a bathroom ($V = 14.1$ [$m^3$], target level = 100 ppm, $T_s = 525$ [s]). Dotted line shows the tracer injection rate (arbitrary units).

b) Air change rates deduced from the CCTG measurement. Large air change rate variations due to the mechanical ventilation system can be observed.

We also tried to use the multizone control algorithm briefly presented in chapter 2.3. The first trial did not improve significantly the control ability. There are two reasons for this result :

- the control matrixes $K_S$ $K_R$ and $K_W$ are diagonally dominant :
  the off-diagonal elements lie one order of magnitude under the diagonal elements which are close to the values of the single zone algorithm.

- The CCTG system is only able to analyze and to dose with tracer gas one zone at a time, which implies that the multizone control algorithm is not completely used. A CCTG system able to analyze and dose many zones simultaneously would take advantage of this multizone algorithm.

Although further work should be useful to refine these findings, it appears that the single zone control algorithm can be used for multizone CCTG system : all zones are simply independently controlled.

## 4. CONCLUSIONS

A complete control algorithm has been developed and the values required to compute its parameters have been systematically investigated. Some improvements of the theoretical algorithm were developed to avoid inappropriate control behaviour due to the physical limitations of the CCTG system.

The presented algorithm is now implemented on our multizone CCTG system CESAR[4,8]. The control algorithm considers each zone independently.

Further work is necessary to develop an automatic parameters recalculation procedure when large variations in air change rate are encountered. The possibility for the algorithm to be extended to a multivariable control algorithm also needs further investigations. It is probable that this algorithm would be useful for multizone CCTG system able to analyze and dose many zones simultaneously.

REFERENCES


1 Bohac D.L., Harrje D.T.
Improving the accuracy of a constant concentration tracer gas system
In 6th AIC Conference "Ventilation strategies and measurement techniques"
1985 (Airbase # 1796)

2 Bohac D.L.
The use of a constant concentration tracer gas system to measure ventilation in buildings
PV/CEES Report N° 205, Princeton Univ., 1986 (Airbase # 2076)

3 Sandberg M., Blomqvist C.
A quantitative estimate of the accuracy of tracer gas methods for the determination of the ventilation flow rate in buildings
In Building and Environment, Vol. 20 N° 3, 1985 (Airbase # 1947)

4 Scartezzini J.-L., Roulet C.-A., Jolliet O.
Continuous air renewal measurements in different inhabited buildings
In 6th AIC Conference "Ventilation strategies and measurement techniques"
1985 (Airbase # 1784)

5 Bühler H.
Réglages échantillonnés (Volume 2 : traitement dans l'espace d'état)
Presses Polytechniques Romandes, Lausanne, 1983.

6 Sherman M.H., Grimsrud D.T., Condon P.E., Smith B.V.
Air infiltration measurement technique
In 1st AIC Conference "Instrumentation and measuring techniques"
1980 (Airbase # 611)

7 Kohler A.
Simulation d'un dispositif de mesure des taux de renouvellement d'air en vue de tester des algorithmes de régulation
Travail de diplôme d'ingénieur physicien, EPFL, 1987

8 Roulet C.-A., Scartezzini J.-L.
Measurement of air change rate in an inhabited building with a constant tracer gas concentration technique
In ASHRAE trans. 93 part 1, 1987.